An Improved Fixed Sphere Decoder Employing Soft Decision for the Detection of Non-orthogonal Signals

Tongyang Xu, Ryan C Grammenos, Farokh Marvasti, and Izzat Darwazeh

***Abstract*—This letter proposes a hybrid soft iterative method together with Fixed Sphere Decoding (FSD) concurrently optimize performance and complexity. We show that for bandwidth compression factors of up to 25 percent, we can achieve the same performance as Orthogonal Frequency Division Multiplexing (OFDM). For systems with bandwidth compression higher than 25 percent, the complexity/performance trade-offs of the hybrid method are better than those of Truncated Singular Value Decomposition-FSD (TSVD-FSD).**

***Index Terms*—Multicarrier communications, spectral efficiency, OFDM, SEFDM, soft decision, iterative detection, fixed sphere decoder.**

I. Introduction

WITH the aim of improving spectrum utilization, non-orthogonal multicarrier technologies have been developed such as Spectrally Efficient Frequency Division Multiplexing (SEFDM) [1][2] and its sister Faster than the Nyquist (FTN) signalling method [3][4]. SEFDM systems employ non-orthogonal overlapped carriers where the spectral efficiency is improved by reducing the spacing between the subcarriers. Therefore, given the same bandwidth allocation SEFDM offers higher throughput than OFDM. The key challenge that arises in SEFDM systems is the self-created interference which gives rise to Inter Carrier Interference (ICI). This interference is caused by the deliberate violation of the orthogonality rule defined for OFDM which requires the frequency spacing to equal the reciprocal of the OFDM symbol period. Therefore, complicated detectors are employed to extract signals from ICI due to the loss of orthogonality [5]. TSVD-FSD [6] was employed for good complexity/performance trade-offs as a practical alternative to optimal Maximum Likelihood (ML) and sub-optimal Sphere Decoding (SD) detections. Work in [7][8][9] adopt iterative methods with Forward Error Control (FEC) decoding to cope with the interference issues. In this work, we propose uncoded hybrid soft Iterative Detection (ID) [10] together with FSD [11] which yields much better complexity/performance trade-offs than the TSVD-FSD detector.

II. SEFDM System Model

The frequency distance between the sub-carriers in SEFDM is defined by $\Delta f = \frac{\alpha}{T}$, where α is the bandwidth compression factor and T is the time duration of one SEFDM symbol. An OFDM signal corresponds to α=1, while for α <1, a normalized SEFDM signal [12] may be represented by the equation below:

$$x(t) = 1/\sqrt{T} \sum_{l=-\infty}^{\infty} \sum_{n=0}^{N-1} s_{l,n} \exp[\frac{j2\pi n\alpha(t-lT)}{T}] \quad (1)$$

where N is the number of sub-carriers and $s_{l,n}$ is the symbol modulated on the n^{th} sub-carrier in the l^{th} SEFDM frame.

The SEFDM signal $x(t)$ in equation (1) is transmitted contaminated with Additive White Gaussian Noise (AWGN) and reaches the receiver as

$$r(t) = x(t) + z(t) \quad (2)$$

where $z(t)$ denotes the AWGN added to the transmitted signal.

The SEFDM reception process can be represented by a discrete model as

$$R = \mathbf{C}S + Z \quad (3)$$

where R is an N-dimensional vector of distorted symbols after demodulating the received symbols using a Fast Fourier Transform (FFT) operation, $\mathbf{C}$ is an $N \times N$ correlation matrix that describes the interferences between the sub-carriers. This matrix is derived by correlating the sub-carriers matrix $\mathbf{F}$ with the conjugate sub-carriers matrix $\mathbf{F}^*$. It is defined as $\mathbf{C} = \mathbf{F}^*\mathbf{F}$, S denotes the N-dimensional vector of transmitted symbols and Z represents the N-dimensional vector of Gaussian noise. The distorted symbols R are finally fed to a detector to generate estimate of the transmitted signal.

III. Soft Iterative SEFDM Detectors

$Notation$: The tree width is denoted by T_W and υ denotes the number of iterations. Matrices are denoted by bold uppercase letters, italic letters represent column vectors.

A. Iterative Detection

Iterative detection algorithms had been used to compensate for the interpolation distortion [13]. Later this technique was applied to nonuniform sampling recovery [14]. A soft version of ID was used for SEFDM in [10]. The main idea of this algorithm is that if a signal κ is distorted by a matrix $\mathbf{G}$ to produce $\gamma = \mathbf{G}\kappa$, then the signal κ can be recovered from the distorted signal γ. This algorithm for SEFDM system is defined by (4).

$$S_n = \lambda R + (e - \lambda\mathbf{C})S_{n-1}, \quad (4)$$

where S_n is an N-dimensional vector of recovered symbols after n iterations, S_{n-1} is an N-dimensional vector of estimated

Manuscript received July 9, 2013. The associate editor coordinating the review of this letter and approving it for publication was M. Lentmaier.

The authors are with the Department of Electronic and Electrical Engineering, University College London, London, UK (e-mail: {tongyang.xu.11, r.grammenos, f.marvasti, i.darwazeh}@ucl.ac.uk).

Digital Object Identifier 10.1109/LCOMM.2013.090213.131573

[1]Prof Marvasti was partially supported by Iran National Science Foundation (INSF).

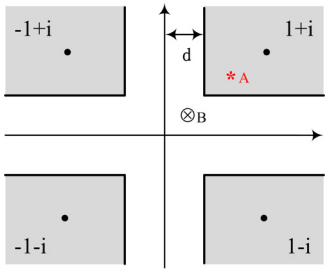

Fig. 1. Soft mapping principle.

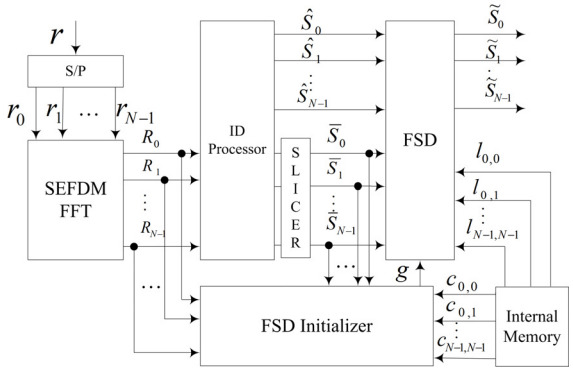

Fig. 2. Block diagram of ID-FSD detector.

symbols after $n-1$ iterations, e is an $N \times N$ identity matrix and λ is a convergence factor, between 1 and 2 that determines how many iterations are used in the detection. In this letter, λ is set to 1. As mentioned in [6], the accuracy of the calculation of the initial estimate determines the ease of approaching the optimal solution. TSVD is a hard mapping detector while ID is effectively a soft iterative method which can be used to generate a more accurate initial estimate relative to the TSVD method discussed in [6]. Soft mapping at each iteration is illustrated in Figure 1. The white uncertainty interval is defined by $d = 1 - \frac{m}{v}$, where m is the m_{th} iteration. Only points that fall in the grey area can be mapped to the corresponding constellation point. Other points are kept unchanged and left to the next iteration. It should be noted that the uncertainty area is reduced after each iteration. The solution should always be found as long as there is a sufficient number of iterations. For example, in Figure 1 point A is mapped to $1+i$ while point B is reserved for the next iteration. Although this soft mapping will significantly reduce the impact of noise the overall performance is still far from optimum.

B. Hybrid ID-FSD Detection

In this section we propose a new hybrid iterative FSD algorithm that is described in Algorithm 1. Figure 2 depicts a block diagram for the new hybrid Iterative Detection-FSD (ID-FSD) detector.

1) ID-Processor: $\hat{S}$ is an N-dimensional vector of unconstrained estimated symbols and at the final iteration stage each symbol is rounded or sliced to the closest integer, thus defines an N-dimensional vector of constrained estimated symbols $\bar{S}$.

Algorithm 1 : Hybrid ID-FSD Detection.

$[\hat{S}, \bar{S}] \Leftarrow ID(R, \mathbf{C}, \lambda, v)$;
$\bar{S} = R$;
for $m = 1; m \leq v; m++$ **do**
  $\hat{S} = \lambda R + (e - \lambda \mathbf{C})\bar{S}$;
  $[\bar{S}] = SoftMapping(\hat{S}, d)$;
  $d = 1 - \frac{m}{v}$;
  $\hat{S}_{\Re} = Real(\hat{S})$, $\hat{S}_{\Im} = Imag(\hat{S})$;
  if $\hat{S}_{\Re} > d \& \hat{S}_{\Im} > d$ **then**
    $\bar{S} = 1 + i$;
  else if $\hat{S}_{\Re} > d \& \hat{S}_{\Im} < -d$ **then**
    $\bar{S} = 1 - i$;
  else if $\hat{S}_{\Re} < -d \& \hat{S}_{\Im} > d$ **then**
    $\bar{S} = -1 + i$;
  else if $\hat{S}_{\Re} < -d \& \hat{S}_{\Im} < -d$ **then**
    $\bar{S} = -1 - i$;
  else
    $\bar{S} = \hat{S}$;
  end if
end for
$[\tilde{S}] \Leftarrow FSD(\hat{S}, \bar{S})$;

$chol\{\mathbf{C}^*\mathbf{C}\} = \mathbf{L}^*\mathbf{L}$;
$D = \left\|R - \mathbf{C}\tilde{S}\right\|^2 = \left\|\mathbf{L}(\hat{S} - \tilde{S})\right\|^2$;
$\breve{s}_n = [1+i, 1-i, -1+i, -1-i]$;
$d = 0$;
for $m = N; m \geq 1; m--$ **do**
  for $n = N; n \geq m; n--$ **do**
    $d = [l_{m,n}(\hat{s}_n - \breve{s}_n)]^2 + d$;
  end for
  if $length(d) > T_W$ **then**
    $d = Sort[d]$;
  else
    $d = d$;
  end if
end for
$AED = min[d]$;
$\breve{g}_{ID} = \left\|R - \mathbf{C}\bar{S}\right\|^2$;
if $AED \leq \breve{g}_{ID}$ **then**
  $\tilde{S}_{ID-FSD} = \tilde{S}$;
else
  $\tilde{S}_{ID-FSD} = \bar{S}$;
end if

2) FSD-Initializer: This block is responsible for generating initial radius $\breve{g}_{ID}$ which determines the size of the search sphere, as in the equation below.

$$\breve{g}_{ID} = \left\|R - \mathbf{C}\bar{S}\right\|^2 \tag{5}$$

where $\|.\|$ denotes the Euclidean norm. The initial radius equals the distance between the sphere center and the initial constrained estimate $\bar{S}$. Due to the ill conditioning of the SEFDM system, these initial estimates may deviate greatly from the optimal points. TSVD was previously applied [6] to cope with this problem. However, the improvement was limited. Therefore, ID is employed here to calculate an improved initial radius.

3) FSD: This block implements the SEFDM detection algorithm using equation:

$$\tilde{S}_{ID-FSD} = \arg \min_{\tilde{S} \in O^N} \left\|R - \mathbf{C}\tilde{S}\right\|^2 \leq \breve{g}_{ID} \tag{6}$$

where $\tilde{S}$ are detected symbols, O is the constellation cardinality and $\breve{g}_{ID}$ is the initial radius transferred from FSD-Initializer. If finally no node is found within the sphere, the ID constrained estimate is taken as the solution $\bar{S}$, as expressed in the equality below:

$$\tilde{S}_{ID-FSD} = \bar{S} \tag{7}$$

This is why the design contains a feed of the constrained estimates from ID-Processor to the FSD block. In order to simplify the squared Euclidean norm calculation, equation (6) can be transformed into an equivalent expression using Cholesky Decomposition. The transformation is carried out using $chol\{\mathbf{C}^*\mathbf{C}\} = \mathbf{L}^*\mathbf{L}$ [6], where $\mathbf{L}$ is an $N \times N$ upper triangular matrix. Hence, (6) can be re-written as

$$\tilde{S}_{ID-FSD} = \arg \min_{\tilde{S} \in O^N} \left\|\mathbf{L}(\hat{S} - \tilde{S})\right\|^2 \leq \breve{g}_{ID} \tag{8}$$

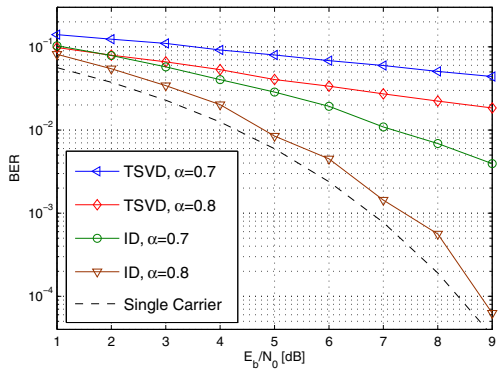

Fig. 3. BER performance for ID and TSVD detectors carrying 4QAM symbols for N=16, υ=20 for T_W=16 with $\alpha = 0{,}7$ and 0.8.

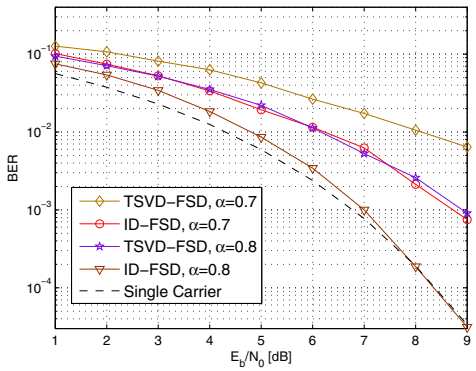

Fig. 4. BER performance for ID-FSD and TSVD-FSD detectors carrying 4QAM symbols for N=16, υ=20 for T_W=16.

4) Internal Memory: The elements of $\mathbf{C}$ and Cholesky decomposition of $\mathbf{C}$ are stored in this block, where $c_{m,n}$ are the elements of $\mathbf{C}$ and are used for calculating the initial radius in equation (5). $l_{m,n}$ denotes the elements of the upper triangular matrix and are used for calculating squared Euclidean norm in equation (8).

IV. Numerical Results

The performance and complexity of the proposed detector are evaluated. The work in this paper is to prove a concept. Therefore, the modulation scheme adopted throughout the simulations is 4-QAM and only an AWGN channel is assumed.

A. Performance

Figure 3 compares the performance of two simplified detectors. The results show that the ID detector outperforms the TSVD one for various bandwidth compression factors.

The purpose of Figure 4 is to demonstrate that ID-FSD is superior to TSVD-FSD for various bandwidth compression factors. More importantly, when $\alpha = 0.8$, the curve is very close to the theoretical one, which indicates the hybrid detector has quasi-optimum performance. It is of interest to note that for low SNR values, there is still nearly 1dB deviation between the ID-FSD and single carrier curves. This is attributed to errors in the initial estimate which come from ID detection in Figure 3. In order to narrow the deviation to zero, we need to increase further the value of tree width (T_W).

Testing for different tree widths, Figure 5 shows that the much lower complexity ID-FSD detector with T_W=16 has a very close performance to that of the TSVD-FSD detector with T_W=1024. Such result is highly encouraging for achieving high performing SEFDM detection with realistic complexity. The complexity issue is further explored below.

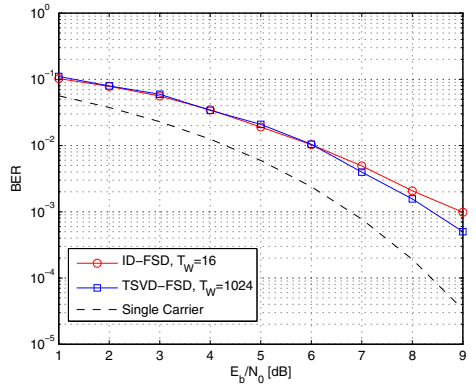

Fig. 5. BER performance for different detectors carrying 4QAM symbols for N=16 , υ=20, α =0.7.

B. Complexity

We represent the complexity in terms of real-valued multiplications and real-valued additions. For this we consider operations for detecting each symbol, not the operations required only once in the detection process (e.g. Singular Value Decomposition for correlation matrix). The complexity of ID is calculated according to equation (4) and the complexity of TSVD can be easily derived. The complexity analysis of FSD is more involved. The computation can be divided into two parts. At the first $\omega = \log_2 T_W$ levels, all the nodes are searched, which means Full Expansion (FE), while for the remaining levels, $2T_W$ nodes are searched and only T_W nodes are reserved, which means Partial Expansion (PE). Furthermore, a sort unit is employed and this consumes more resources. Detailed calculation of complexities yields the results summarised in Table I. The complexity is analyzed in detail for implementation on an FPGA platform in [15].

Table II shows normalised delay comparison of both ID-FSD and TSVD-FSD detectors. Assuming both ID-FSD (N=16,υ=20) and TSVD-FSD (N=16) employ parallel and pipelined structures. Regarding initial delay, ID-FSD consumes 19 more clock cycles than TSVD-FSD. In terms of pipelined delay, both schemes consume one clock cycle.

Figure 6 illustrates the MATLAB execution time of different detectors and for various iterations and tree widths. We use the execution time to compare the relative complexity of detectors. The figure clearly shows the new ID-FSD detector, even with a very high number of iterations, always displays execution time one order of magnitude lower than its TSVD-FSD counterpart. This trend is consistent with the absolute numbers of Table I. It is obvious that TSVD-FSD detector needs more computational

TABLE I
COMPLEXITY COMPARISONS

	TSVD	ID	FSD
Number of Multiplication Operations	$4N^2$	$4\upsilon N^2$	$\underbrace{\sum_{n=1}^{\omega} 2^n[2n+1]}_{FE} + \underbrace{\sum_{m=\omega+1}^{2N} T_W[2m+1]}_{PE}$
Number of Addition Operations	$4N^2-2N$	$8\upsilon N^2$	$\underbrace{\sum_{n=1}^{\omega} 2^n[2n-1]}_{FE} + \underbrace{\sum_{m=\omega+1}^{2N} T_W[2m-1]}_{PE} + \underbrace{4{T_W}^2(2N-\omega)}_{sort}$
Number of Operations: TSVD-FSD(N=16, T_W=1024)	2016		94285832
Number of Operations: ID-FSD(N=16, T_W=16, υ=20)		61440	62216

TABLE II
DELAY COMPARISONS (NORMALISED VALUES)

	TSVD	ID	FSD
Initial Delay(Clock Cycles)	1	υ	N
υ=20,N=16	1	20	16
Pipelined Delay(Clock Cycles)	1	1	1

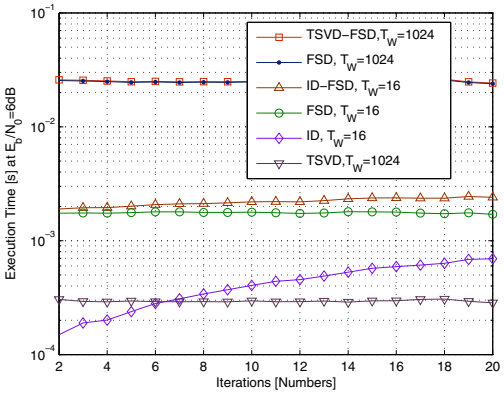

Fig. 6. Execution time versus iteration numbers for different SEFDM detectors carrying 4QAM symbols with $\alpha = 0.7$, N=16.

operations than ID-FSD detector. As a result, the ID-FSD detector takes significantly less time than TSVD-FSD detector to complete a detection.

V. CONCLUSIONS

In this letter, we show that up to 25 percent spectral efficiency gain is a realistic option for non-orthogonal multi-carrier systems. A new detector combining ID with FSD was developed and its performance assessed through simulations. The new ID-FSD detector achieves quasi-optimum performance at realistic complexity, the latter being nearly a 10% of the complexity of a similar performance TSVD-FSD detector. For different bandwidth compression factors, the performance/complexity behavior of the new technique is the best achieved so far.

VI. ACKNOWLEDGEMENT

The authors sincerely thank Mr Javad Heydari for providing the Iterative Detector software.

REFERENCES

[1] I. Kanaras, A. Chorti, M. Rodrigues, and I. Darwazeh, "Spectrally efficient FDM signals: bandwidth gain at the expense of receiver complexity," in *Proc. 2009 IEEE International Conference on Communications*, pp. 1–6.

[2] R. Clegg, S. Isam, I. Kanaras, and I. Darwazeh, "A practical system for improved efficiency in frequency division multiplexed wireless networks," *IET Commun.*, vol. 6, no. 4, pp. 449–457, 2012.

[3] J. Anderson, F. Rusek, and V. Owall, "Faster-than-nyquist signaling," *Proc. IEEE*, vol. 101, no. 8, pp. 1817–1830, 2013.

[4] F. Rusek and J. Anderson, "Multistream faster than nyquist signaling," *IEEE Trans. Commun.*, vol. 57, no. 5, pp. 1329–1340, 2009.

[5] R. C. Grammenos and I. Darwazeh, "Performance trade-offs and DSP evaluation of spectrally efficient FDM detection techniques," in *2013 IEEE Int.Conf. Commun.*

[6] S. Isam, I. Kanaras, and I. Darwazeh, "A truncated SVD approach for fixed complexity spectrally efficient FDM receivers," in *2011 IEEE Wireless Commun. and Networking Conf.*

[7] B. Beidas, H. El-Gamal, and S. Kay, "Iterative interference cancellation for high spectral efficiency satellite communications," *IEEE Trans. Commun.*, vol. 50, no. 1, pp. 31–36, 2002.

[8] G. Colavolpe, D. Fertonani, and A. Piemontese, "SISO detection over linear channels with linear complexity in the number of interferers," *IEEE J. Sel. Topics Signal Process.*, vol. 5, no. 8, pp. 1475–1485, 2011.

[9] A. Barbieri, D. Fertonani, and G. Colavolpe, "Time-frequency packing for linear modulations: spectral efficiency and practical detection schemes," *IEEE Trans. Commun.*, vol. 57, no. 10, pp. 2951–2959, 2009.

[10] S. Heydari, M. Ferdosizadeh, and F. Marvasti, "Iterative detection with soft decision in spectrally efficient FDM systems," Tech. Rep. arXiv:1304.4003v1, Apr. 2013.

[11] L. Barbero and J. Thompson, "Rapid prototyping of a fixed-throughput sphere decoder for MIMO systems," in *Proc. 2006 IEEE International Conference on Communications*, vol. 7, pp. 3082–3087.

[12] M. Rodrigues and I. Darwazeh, "A spectrally efficient frequency division multiplexing based communications system," in *Proc. 2003 Int. OFDM Workshop*, pp. 48–49.

[13] F. Marvasti, "An iterative method to compensate for the interpolation distortion," *IEEE Trans. Acoust., Speech, Signal Process.*, vol. 37, no. 10, pp. 1617–1621, 1989.

[14] F. Marvasti, M. Analoui, and M. Gamshadzahi, "Recovery of signals from nonuniform samples using iterative methods," *IEEE Trans. Signal Process.*, vol. 39, no. 4, pp. 872–878, 1991.

[15] T. Xu, R. C. Grammenos, and I. Darwazeh, "FPGA implementations of real-time detectors for a spectrally efficient FDM system," in *2013 IEEE Int, Conf. Telecommun.*